

Functional Mitochondrial Complex I Is Required by Tobacco Leaves for Optimal Photosynthetic Performance in Photorespiratory Conditions and during Transients¹

Christelle Dutilleul, Simon Driscoll, Gabriel Cornic, Rosine De Paepe, Christine H. Foyer, and Graham Noctor*

Institut de Biotechnologie des Plantes (C.D., R.D.P., G.N.) and Laboratoire d'Ecophysiologie Végétale (G.C.), Université de Paris XI, 91405 Orsay cedex, France; and Crop Performance and Improvement Division, Rothamsted Research, Harpenden, Hertfordshire AL5 2JQ, United Kingdom (S.D., C.H.F.)

The importance of the mitochondrial electron transport chain in photosynthesis was studied using the tobacco (*Nicotiana sylvestris*) mutant CMSII, which lacks functional complex I. Rubisco activities and oxygen evolution at saturating CO₂ showed that photosynthetic capacity in the mutant was at least as high as in wild-type (WT) leaves. Despite this, steady-state photosynthesis in the mutant was reduced by 20% to 30% at atmospheric CO₂ levels. The inhibition of photosynthesis was alleviated by high CO₂ or low O₂. The mutant showed a prolonged induction of photosynthesis, which was exacerbated in conditions favoring photorespiration and which was accompanied by increased extractable NADP-malate dehydrogenase activity. Feeding experiments with leaf discs demonstrated that CMSII had a lower capacity than the WT for glycine (Gly) oxidation in the dark. Analysis of the postillumination burst in CO₂ evolution showed that this was not because of insufficient Gly decarboxylase capacity. Despite the lower rate of Gly metabolism in CMSII leaves in the dark, the Gly to Ser ratio in the light displayed a similar dependence on photosynthesis to the WT. It is concluded that: (a) Mitochondrial complex I is required for optimal photosynthetic performance, despite the operation of alternative dehydrogenases in CMSII; and (b) complex I is necessary to avoid redox disruption of photosynthesis in conditions where leaf mitochondria must oxidize both respiratory and photorespiratory substrates simultaneously.

Plant biomass production is ultimately determined by the ratio between photosynthesis and respiratory CO₂ release, and 30% to 70% of fixed carbon can be rereleased within each 24-h cycle (Lambers, 1997). Therefore, manipulation of respiration is a potential approach to improving agricultural yields (Lewis et al., 2000). One current difficulty is that, quite apart from the roles played by respiration in heterotrophic tissues, the importance of leaf respiration for the process of carbon fixation itself is not yet fully established. Leaf mitochondria may have several functions during photosynthesis (for review, see Krömer, 1995; Hoefnagel et al., 1998; Gardeström et al., 2002). These include oxidation of malate generated by the photosynthetic electron transport chain (Backhausen et al., 1998), production of organic acids for chloroplastic ammonia assimilation (Foyer et al., 2001), and generation of ATP to support UDP-Glc formation for Suc synthesis (Krömer et al., 1988, 1993). A key function of leaf mitochondria during photosynthesis, particularly in C₃ species, is the oxidation of Gly produced in the photorespiratory pathway (Douce

and Neuburger, 1989) through reactions catalyzed by Gly decarboxylase (GDC) and Ser hydroxymethyl transferase, enzymes found in abundance in the mitochondrial matrix (Oliver et al., 1990). Although the importance of these enzymes in photorespiratory carbon recycling is well established (Somerville and Ogren, 1981; Blackwell et al., 1990; Heineke et al., 2001), and although isolated mitochondria show high rates of Gly-linked O₂ consumption (e.g. Krömer and Heldt, 1991), the role of the mitochondrial electron transport chain during whole-leaf photorespiration remains unclear (Leegood et al., 1995; Foyer and Noctor, 2000).

Data on mitochondrial roles in photosynthesis have largely been produced either by analysis of isolated organelles or by using inhibitors. Evaluation of the physiological roles of mitochondrial electron transport is complicated by the existence in plants of several NAD(P) H dehydrogenases and an alternative terminal oxidase, in addition to cytochrome oxidase (Møller, 2001). Definitive assessment of the in vivo role of the mitochondrial electron chain in photosynthetic metabolism is limited by the scarcity of available mutants with specific genetic lesions in key components. Such mutants are likely to yield key insights into the roles of mitochondrial electron transport components in vivo, and their importance or redundancy in given conditions. Antisense technology has been used to decrease alternative oxidase

¹ This work was supported by the European Union and by the British Council ALLIANCE/French Ministry of Education EGIDE grant for exchange between French and UK researchers.

* Corresponding author; e-mail noctor@ibp.u-psud.fr; fax 33-1-69-15-34-25.

Article, publication date, and citation information can be found at www.plantphysiol.org/cgi/doi/10.1104/pp.011155.

expression in tobacco (*Nicotiana tabacum*) and the consequences for leaf respiration have been investigated (Vanlerberghe et al., 1994). To date, however, no thorough analysis has appeared of the effects on photosynthesis of genetic decreases in components of the mitochondrial electron transport chain.

A decreased photosynthesis to respiration ratio was reported recently in the *Nicotiana sylvestris* mutant, CMSII, in which the major mitochondrial NADH dehydrogenase, complex I, is nonfunctional (Sabar et al., 2000). CMSII carries a lesion in the mitochondrion-encoded gene *NAD7*, encoding a key complex I component (Gutierrez et al., 1997). The mutant grows more slowly than wild-type (WT) plants, but is ultimately able to sustain similar biomass production because of the operation of alternative mitochondrial dehydrogenases. Studies of the respiratory capacities of isolated CMSII mitochondria showed that the mutant has a capacity for malate and succinate oxidation that is similar to the WT, that O₂ consumption in CMSII mitochondria is rotenone-insensitive, and that CMSII mitochondria catalyze increased rates of oxidation of external NADH (Gutierrez et al., 1997; Sabar et al., 2000). Isolated CMSII mitochondria, however, have a capacity for Gly-linked O₂ uptake that is less than 30% of the WT (Gutierrez et al., 1997; Sabar et al., 2000). Therefore, this mutant presents an excellent system in which to examine the role of the mitochondrial electron transport chain in supporting the complex energetic interactions between different compartments during C₃ photosynthesis. In this study, we have analyzed the conditions in which mitochondrial complex I function is necessary for whole-leaf photosynthesis. It is shown that CMSII has a similar photosynthetic capacity to WT tobacco, but that photosynthesis is nevertheless disrupted in physiological conditions, notably when net carbon fixation and photorespiration are simultaneously active and, most strikingly, during dark-light transients. It is concluded that in these conditions, complex I is required to allow efficient redox exchange between compartments and to avoid

Table I. Rates of respiration and maximum photosynthesis in *N. sylvestris* WT and the CMSII mutant

Oxygen exchange was measured in a leaf disc oxygen electrode, where CO₂ is maintained at saturating partial pressure (approximately 30 mbar). To drive maximum rates of photosynthetic O₂ evolution, irradiance was 1,400 μmol m⁻² s⁻¹. O₂ exchange data are means ± SE of three leaf discs, each from a different plant. CO₂ release was measured in attached leaves by infrared gas analysis at 350 μbar CO₂, 20 min after introduction of the leaf into the chamber and darkening. CO₂ evolution data are means ± SE of 18 (WT) and 10 (CMSII) measurements of attached leaves.

Measurement	WT	CMSII
	μmol m ⁻² leaf surface s ⁻¹	
Photosynthetic O ₂ evolution	33.1 ± 2.0	36.4 ± 3.8
Respiratory O ₂ consumption	1.29 ± 0.29	2.14 ± 0.48
Respiratory CO ₂ evolution	1.12 ± 0.18	1.87 ± 0.16

Table II. Amounts and activities of Rubisco in tobacco WT and the CMSII mutant

Samples were taken from plants dark adapted for 5 h (dark) or illuminated at an irradiance of 700 μmol m⁻² s⁻¹ for 2 h (light). Initial, total, and maximal activities are expressed as μmol CO₂ min⁻¹ μmol⁻¹ Rubisco. Total Rubisco catalytic sites are expressed as nmol Rubisco mg⁻¹ chlorophyll. For details, see "Materials and Methods." Data are means ± SE of samples from four different plants.

Measurement	WT	CMSII
Total catalytic sites		
Dark	42 ± 2	56 ± 4
Light	42 ± 2	56 ± 2
Initial activity		
Dark	33 ± 2	29 ± 2
Light	134 ± 5	135 ± 4
Total activity		
Dark	69 ± 6	77 ± 4
Light	130 ± 3	132 ± 3
Maximal activity		
Dark	125 ± 3	125 ± 3
Light	121 ± 2	122 ± 4

over-reduction of the photosynthetic system. Despite the well-known redundancy of leaf metabolism, and the existence of several alternative dehydrogenases in the mitochondrial electron transport chain, complex I is indispensable in conferring on the photosynthetic system the flexibility needed to cope with environmental changes such as fluctuations in irradiance and water availability.

RESULTS

Photosynthetic Capacity in the CMSII Mutant Is at Least as High as in the WT

Although CMSII lacks functional complex I, dark rates of respiratory O₂ consumption and CO₂ release were increased by 60% to 70% compared with the WT (Table I). Maximum net photosynthetic O₂ evolution in tobacco requires a CO₂ partial pressure greater than 5 mbar to completely suppress ribulose 1,5-bisphosphate (RuBP) oxygenation (Ruuska et al., 2000). Therefore, light-dependent O₂ evolution was measured in an O₂ electrode chamber where CO₂ is maintained at around 30 mbar. At this partial pressure, and at high irradiance, light-dependent O₂ evolution was rapidly induced (within 10 min) in both types of plant to give rates similar to those previously reported for *Nicotiana tabacum* leaves (Ruuska et al., 2000). Steady-state rates were marginally higher, on a leaf area basis, in the mutant (Table I).

Expressed relative to chlorophyll, Rubisco contents were about 30% higher in the mutant (Table II). No difference was found between the two genotypes in Rubisco activities per unit Rubisco protein (Table II). In both plants, illumination increased the initial activities (measured without in vitro activation or treatment to remove tight-binding inhibitors) about 4-fold, so that initial activities were equal to total and

maximal activities in illuminated leaves (Table II). Because in vitro activation by carbamylation (total activities and dark) only partly simulated the effect of light, whereas maximal activities were similar in light and dark, the effect of light was apparently because of carbamylation and release of tight-binding inhibitors.

Prolonged Induction of Photosynthesis in CMSII

Under physiological conditions, CMSII showed consistently lower steady-state rates of net CO₂ uptake than the WT (see below). Moreover, the rate of induction of photosynthesis was significantly slower in the mutant (Fig. 1). This effect was reproducible and was observed whether rates of net CO₂ uptake were expressed on a leaf area basis (Fig. 1, main panels) or normalized to the final rate attained by each plant (Fig. 1, insets). The slow induction in CMSII was exacerbated at subatmospheric CO₂ partial pressure (Fig. 1B). Induction kinetics in WT plants were not significantly affected by the difference in CO₂ partial pressure: At both atmospheric and subatmospheric CO₂, photosynthesis reached the steady state in 30 min (Fig. 1). In both conditions, but especially at lower CO₂, an initial induction of CO₂ uptake in the mutant within the first 2 to 5 min was followed by a much slower increase in net CO₂ uptake than in the WT, showing that the absence of complex I imposes a clear restriction on the operation of photosynthesis (Fig. 1).

In a further experiment at subatmospheric CO₂, net CO₂ uptake, transpiration, and intercellular CO₂ concentration were monitored before freeze clamping of samples and determination of stromal NADP-malate dehydrogenase (MDH) activities as a marker for the reduction state of the chloroplast stroma (Fig. 2). The

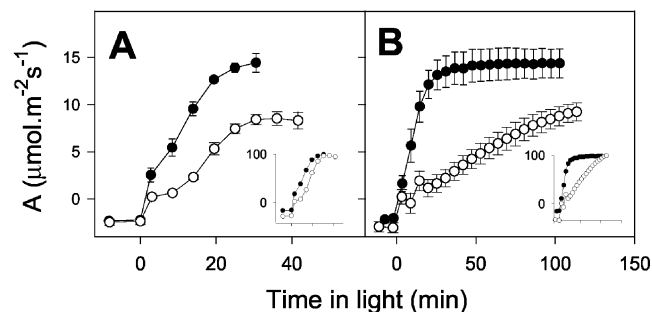


Figure 1. Mitochondrial complex I deficiency is associated with delayed induction of photosynthesis in the CMSII mutant. Black circles, WT. White circles, CMSII. A, Ambient CO₂ = 360 μbar. B, Ambient CO₂ = 250 μbar. In both cases, irradiance was 700 μmol m⁻² s⁻¹ and O₂ pressure was 210 mbar. Insets show net CO₂ exchange normalized to the final values attained by each plant (plotted on same x axis scale as non-normalized rates). Data are means ± SE of three different attached leaves. Where not apparent, error bars are contained within the symbols. The experiments were carried out with separate sets of plants. Similar results were obtained in two other experiments with different sets of plants.

slow onset of photosynthesis in the mutant (Fig. 2A) was accompanied by a slow increase in transpiration (Fig. 2B). However, the relationship between photosynthesis and transpiration was different in the CMSII and the WT, the mutant showing a lower rate of net CO₂ uptake for a given rate of transpiration throughout the induction period (Fig. 2B, inset, compare white and black circles). During the early part of the induction period, intercellular partial pressure of CO₂ (C_i) values were maintained significantly higher in the mutant than in the WT (Fig. 2C). Initial and maximal NADP-MDH activities were very similar to those extractable from pea (*Pisum sativum*) and potato (*Solanum tuberosum*) leaves (Foyer et al., 1992; Backhausen et al., 1998). The mutant showed slightly higher maximal activities, which were not significantly different in light and dark in either plant (Fig. 2E). Although the initial NADP-MDH activity was rapidly light induced in both types of plant, initial activity subsequently decreased in the WT but remained high in the mutant (Fig. 2D).

Photosynthetic Rates in CMSII and WT Tobacco Show a Different Dependence on CO₂ Partial Pressure

Given the marked effects of lower CO₂ partial pressure on the induction kinetics in the mutant, we compared steady-state photosynthesis in the WT and mutant at different CO₂ partial pressures. In the WT, net CO₂ uptake showed a typical hyperbolic dependence on C_i, whereas the curve shape in CMSII was quite different, with a significant break around C_i = 200 to 300 μbar CO₂ (Fig. 3A). As C_i increased to over 600 μbar (ambient CO₂ of approximately 1,000 μbar), the mutant showed a much more evident stimulation of net CO₂ uptake than the WT (Fig. 3A). The result was that rates of photosynthesis at C_i greater than 600 μbar CO₂ were not significantly different in CMSII and the WT (Fig. 3A). During these steady-state analyses, the two types of plant showed an identical relationship between transpiration and net CO₂ uptake as a function of C_i (Fig. 3B).

Complex I Deficiency Does Not Directly Perturb Glycine Metabolism in Illuminated Leaves

The mitochondrial conversion of Gly to Ser, a key step in photorespiratory carbon and nitrogen recycling, requires a sink for NADH produced in the matrix (Leegood et al., 1995). Photorespiration-linked decrease of photosynthesis in the mutant could be because of direct redox control of GDC activity, given that the redox state of the mitochondrial NAD pool is considered a potentially important factor exerting control over GDC activity in vivo (Douce and Neuburger, 1989). Therefore, it is possible that photosynthesis is slowed in CMSII under photorespiratory conditions because of restriction on GDC activ-

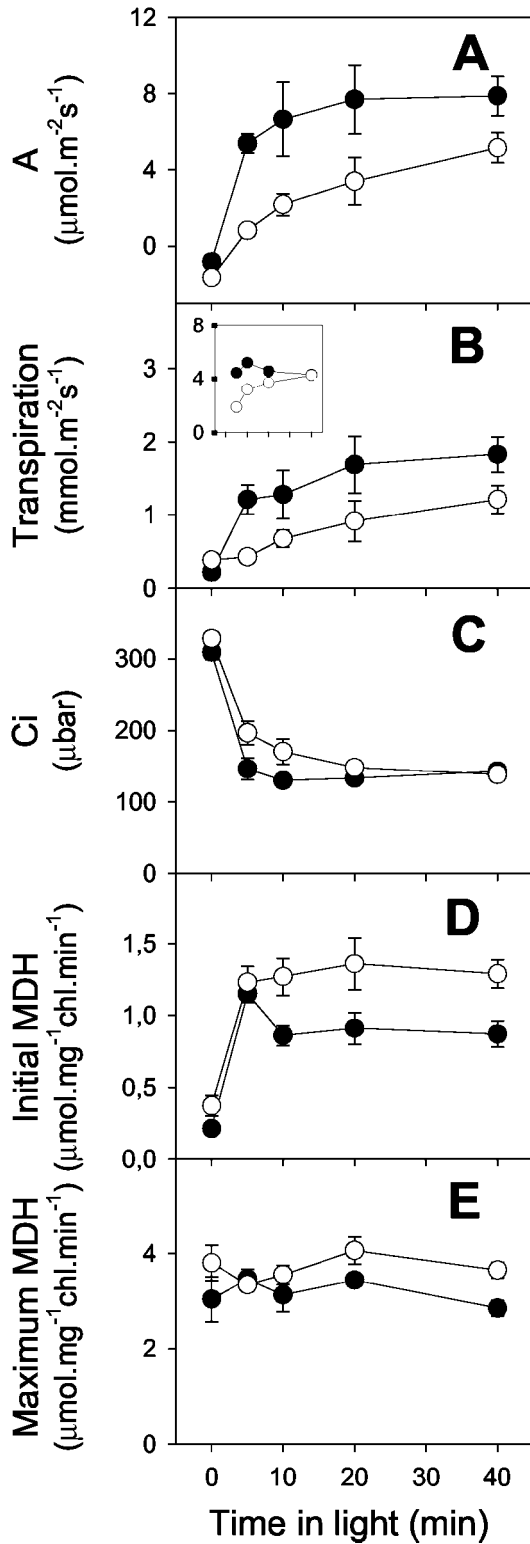


Figure 2. Gas exchange and NADP-MDH activities in attached leaves from WT and CMSII tobacco during the induction period of photosynthesis. Black circles, WT. White circles, CMSII. Plants were dark adapted for 60 min, then illuminated at $700 \mu\text{mol m}^{-2} \text{s}^{-1}$, 210 mbar O_2 , and 250 μbar CO_2 before metabolism was stopped by freeze clamping samples for MDH assays. Each data point is the mean \pm SE of a different set of four plants. A, Net CO_2 uptake; B, transpiration (the

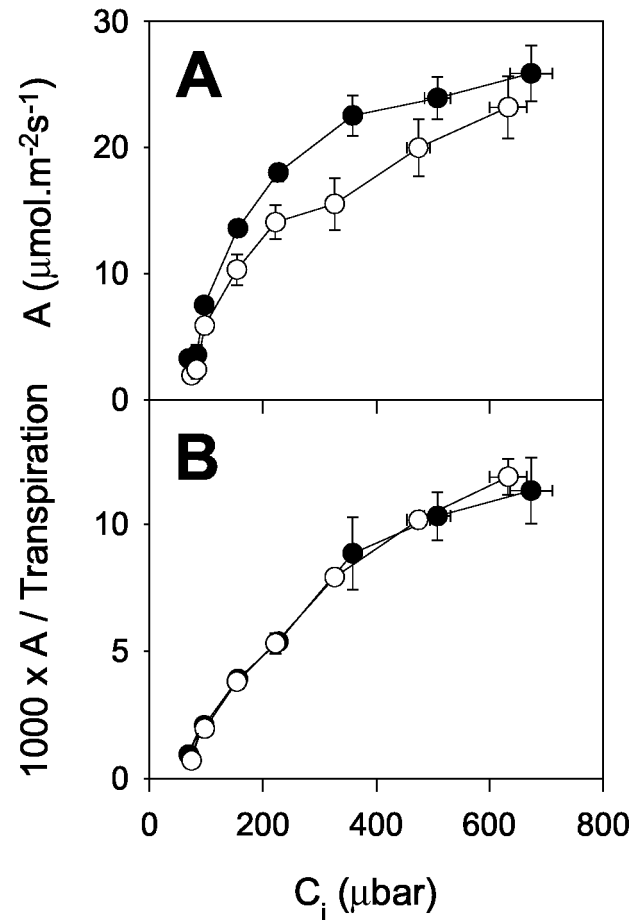


Figure 3. C_i curves for photosynthesis in CMSII and WT tobacco. Black circles, WT. White circles, CMSII. A, Net CO_2 uptake. B, Net CO_2 uptake divided by transpiration. Gas exchange was measured on attached leaves illuminated at 210 mbar O_2 and ambient CO_2 varying from 70 to 1,000 μbar at an irradiance of $700 \mu\text{mol m}^{-2} \text{s}^{-1}$. Data are means \pm SE of four to 16 plants. Where not apparent, error bars are contained within the symbols.

ity, which increases control over carbon recycling to the Calvin cycle. A flux restriction at this enzyme is known to increase the Gly to Ser ratio at a given rate of photorespiration, both in mutants with very low GDC capacity (Blackwell et al., 1990) and in heterozygous plants with intermediate activities (Wingler et al., 1997). Therefore, we compared Gly to Ser ratios in the two genotypes under conditions of widely varying photorespiratory flux. Figure 4 shows data from an experiment where gas exchange was measured at different CO_2 partial pressure, before sampling the incubated portion of the leaf for determination of Gly and Ser. An almost identical relationship was observed between C_i and ambient CO_2 in the mutant and WT (Fig. 4A), suggesting that C:O values at

inset shows 1,000 \times net CO_2 uptake/transpiration, plotted on the same x axis scale as the main panel); C, intercellular CO_2 concentration; D, initial MDH activity; E, maximum MDH activity.

Rubisco were not significantly different in the two genotypes at a given CO_2 partial pressure. Although Gly/Ser displayed a general decrease in both genotypes with increasing ambient CO_2 partial pressure, the ratio was not increased in the mutant compared with the WT (Fig. 4C). Gly/Ser was generally lower in CMSII than in the WT (Fig. 4C). When the relationship between Gly/Ser and net CO_2 uptake was plotted against ambient CO_2 , no difference was observed between the genotypes (Fig. 4C, inset), i.e. Gly/Ser was decreased in the mutant in proportion to the rate of photosynthesis. We conclude that the relationship between the rate of photorespiration and Gly/Ser was not different in the two plant types, and, thus, that complex I deficiency does not directly perturb photorespiratory Gly recycling through GDC. This interpretation is confirmed by the dependence of Gly/Ser on irradiance (Fig. 5). As previously reported (Sabar et al., 2000), net CO_2 uptake was decreased in the mutant to a similar extent at all irradiances (data not shown). In both plants, Gly/Ser increased markedly with irradiance, as observed in other C_3 species (Novitskaya et al., 2002). The ratio was more than 10-fold higher in leaves at high light than in darkened leaves (Fig. 5A). At all irradiances, however, the ratio was lower in CMSII than in the WT (Fig. 5A). When Gly/Ser was plotted against net CO_2 uptake, a similar relationship was observed in both genotypes (Fig. 5B).

Because increased ambient CO_2 alleviated the inhibition of net CO_2 uptake in the mutant (Figs. 3 and 4B), we compared the effect of low O_2 on net CO_2 uptake in the two genotypes. Oxygen sensitivity is a good indicator of excess photosynthetic capacity in C_3 plants (Leegood and Furbank, 1986; Sharkey et al., 1986). At atmospheric O_2 , in agreement with the data in Figures 3 and 4, net CO_2 fixation was about 30% lower in CMSII than in the WT (Table III). In both types of plant, low O_2 stimulated net CO_2 uptake and caused a marked decrease in Gly/Ser, consistent with the expected decrease in photorespiratory flux (Table III). Thus, both genotypes displayed O_2 sensitivity under the experimental conditions. However, the stimulation of photosynthesis by low O_2 was greater in the mutant than in the WT (Table III). This effect is consistent with the data of Table I and Figures 3 and 4, and confirms that the inhibition of net

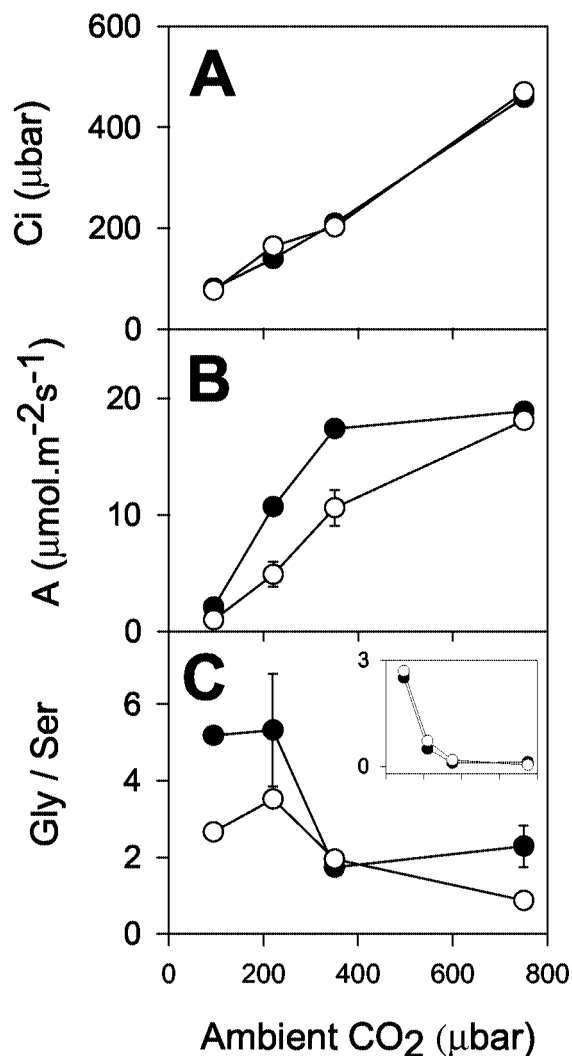


Figure 4. The inhibition of photosynthesis in CMSII in photorespiratory conditions is not associated with increased Gly/Ser. Black circles, WT. White circles, CMSII. A, Intercellular CO_2 concentration. B, Net CO_2 uptake. C, Gly/Ser. The inset shows the ratio between Gly/Ser and the rate of net CO_2 uptake, calculated from data shown in B and C. Values are means of two independent measurements at each condition. Error bars show actual values and are contained within the symbols where not apparent.

Table III. The effect of low O_2 on photosynthesis, transpiration, and Gly/Ser in WT and CMSII leaves

Attached leaves from four WT or CMSII plants were illuminated at an irradiance of $700 \mu\text{mol m}^{-2} \text{s}^{-1}$ and $350 \mu\text{bar CO}_2$, 210 mbar O_2 to induce photosynthesis (30-min illumination). Oxygen was either maintained at 210 mbar or decreased to 20 mbar . After a further 30-min illumination, CO_2 uptake (A) and transpiration were measured, then metabolism was rapidly quenched in the incubated portion of the leaf by freeze clamping. Gly and Ser were extracted and determined by HPLC. Data are means \pm SE.

Plant	WT	WT	CMSII	CMSII
O_2 (mbar)	210	20	210	20
A ($\mu\text{mol m}^{-2} \text{s}^{-1}$)	13.9 ± 0.6	19.6 ± 1.8	9.9 ± 1.4	16.3 ± 1.6
O_2 stimulation of A (%)	–	41	–	65
$1,000 \times \text{A/Transpiration}$	8.2 ± 0.8	11.3 ± 1.7	8.6 ± 0.8	11.6 ± 0.7
Gly/Ser	4.18 ± 0.69	1.31 ± 0.54	2.42 ± 0.19	0.43 ± 0.03

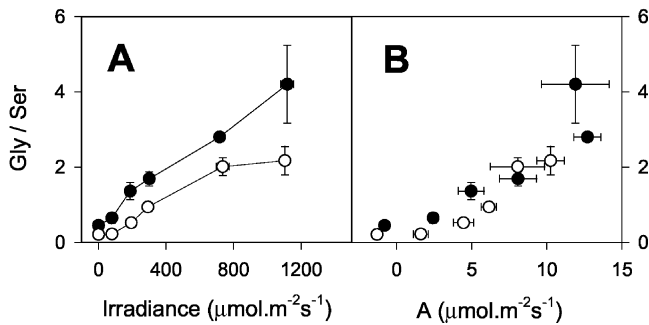


Figure 5. Effect of irradiance on Gly/Ser in CMSII and WT leaves. Black circles, WT. White circles, CMSII. A, Gly/Ser against irradiance. B, Relationship between Gly/Ser and net CO_2 uptake. Attached leaves were illuminated at the irradiance indicated (210 mbar O_2 , 360 μbar CO_2 , 22°C) until the steady-state rate of net CO_2 fixation was reached. Samples were then taken for analysis of Ser and Gly by freeze clamping. Data are means \pm SE of four different plants. Where not apparent, error bars are contained within the symbols.

CO_2 uptake in the mutant is mitigated by suppression of photorespiration. Despite these observations, however, no evidence was found for direct perturbation of Gly metabolism in the mutant. As in the experiments where photorespiratory flux was manipulated by ambient CO_2 and irradiance, Gly/Ser was lower in the mutant than in the WT at each O_2 partial pressure (Table III).

Gly Metabolism in Darkened Leaves Is Slowed in the Absence of Functional Complex I

Isolated CMSII mitochondria have a decreased capacity for Gly oxidation (Sabar et al., 2000). Therefore, we examined whether Gly metabolism was affected in CMSII leaves in the dark, where the mitochondrial electron transport chain is the major sink for NADH produced in the mitochondrial matrix. Figure 6 shows how feeding Gly to leaf discs in the dark affected leaf Gly, Ser, and the product to substrate ratio (Ser/Gly). A high Gly concentration was used together with small leaf discs to maximize the rate of Gly entry into the leaf mitochondria. In discs from the WT, Gly accumulated gradually to 3 $\mu\text{mol mg}^{-1}$ chlorophyll (Fig. 6A), whereas leaf contents of Ser rapidly attained more than twice this value (Fig. 6B). In CMSII discs, however, the accumulation of Ser was significantly slower than in WT discs (Fig. 6B) and Gly continued to accumulate to levels more than 2-fold higher than those found in the WT (Fig. 6A). After 24-h incubation on Gly, WT discs had 3-fold higher Ser/Gly values than discs incubated without Gly, but the ratio in the CMSII discs was not affected by supplying Gly (Fig. 6C). After 24-h incubation, the Ser to Gly ratio in CMSII discs incubated with Gly was similar to discs from both lines incubated in the absence of Gly (Fig. 6C).

Postillumination CO_2 Release in CMSII and the WT

The above analyses suggest that the capacity for Gly metabolism is decreased in CMSII leaves in the dark but not in the light. Therefore, we compared the kinetics of CO_2 evolution immediately after a light/dark transition. Photosynthesis was induced at high

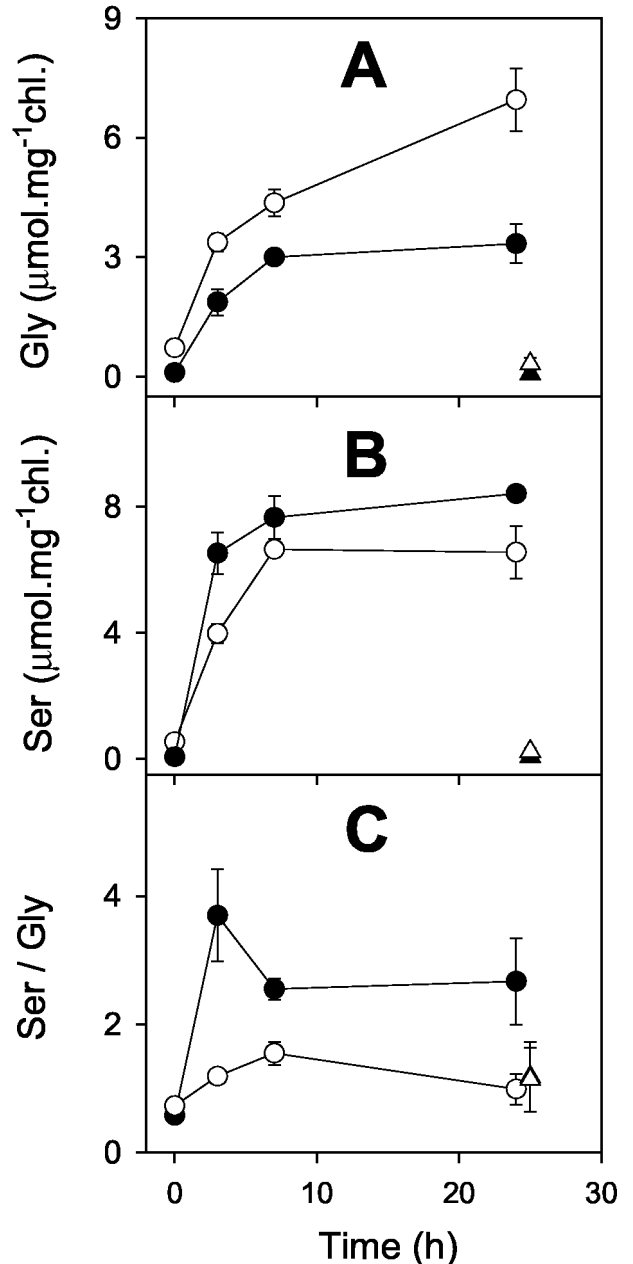


Figure 6. Leaf discs from CMSII convert Gly to Ser in the dark at lower rates than do WT leaf discs. Black circles, WT. White circles, CMSII. Discs were supplied with 50 mM Gly and 5 mM HEPES (pH 7.0), incubated at room temperature in the dark, and samples were taken at the time indicated for analysis of Ser and Gly. For further details, see "Materials and Methods." Triangles show data for discs maintained in the dark on 5 mM HEPES (pH 7.0). Data are means \pm SE of three samples, each composed of eight discs. Where not apparent, error bars are contained within the symbols.

light and 200 $\mu\text{bar CO}_2$ to drive high rates of photorespiration. On darkening, very similar kinetics of CO_2 release were observed in the two genotypes over the first 3 min (Fig. 7). Thus, despite the clear restriction over GDC activity in darkened leaves supplied with Gly, this enzyme is not subject to stricter control in the CMSII mutant during depletion of photorespiratory pools following a light/dark transition. In CMSII, however, the initial burst was followed by a secondary prolonged burst of CO_2 release, between 3 and 12 min after darkening, that was much less evident in the WT leaves (Fig. 7), suggesting either a secondary phase of Gly decarboxylation or metabolism of respiratory substrates that accumulate in CMSII leaves in the light.

DISCUSSION

Loss of complex I function in tobacco does not inhibit leaf respiration measured in the dark. In fact, rates were significantly higher in the mutant, whether determined as CO_2 evolution or O_2 uptake (Table I). This shows that alternative electron transport components are able to substitute for complex I in carbon oxidation. The higher respiration rates in CMSII leaves are associated with engagement of rotenone-insensitive dehydrogenases and decreased sensitivity of respiration to cyanide, suggesting increased activity of the alternative oxidase (Sabar et al., 2000). Given that dark respiration is at least partly inhibited in the light (Krömer, 1995; Pärnik and Keer-

berg, 1995), it is clear that the mutant has a respiratory capacity that is sufficient to cope with carbon oxidation during photosynthesis. Despite this, photosynthesis is significantly inhibited in the mutant in physiological conditions, and particularly during transients. Because dark respiration rates are increased in the mutant, part of the decrease in net CO_2 uptake may possibly be attributed to higher rates of CO_2 release in the light. This effect may contribute to the decrease in photosynthesis when net CO_2 uptake is slow, e.g. low ambient CO_2 and low light. However, increased "day" respiration in the light in CMSII cannot explain the appreciable difference in net CO_2 uptake when photosynthesis is rapid (e.g. $C_i = 200\text{--}360 \mu\text{bar CO}_2$), and the irradiance independence of the decrease in photosynthesis also shows that other mechanisms are operating that perturb net CO_2 uptake in the mutant. Data in this manuscript allow the following conclusions to be drawn.

Decreased Photosynthesis in CMSII Is Not Because of Diminished Photosynthetic Capacity, Effects on Stomatal Function, or Lowered ATP Supply for Suc Synthesis

It is clear from the present study that the lower rates of photosynthesis observed in CMSII at physiological CO_2 concentrations are not because of long-term changes that confer lower photosynthetic capacity on the mutant. Maximal Rubisco activities in the light were around $120 \mu\text{mol CO}_2 \text{ min}^{-1} \mu\text{mol}^{-1}$ Rubisco protein in both genotypes (Table II). Given the differences in Rubisco contents (Table II), these activities convert to CO_2 fixation capacities of 302 and $403 \mu\text{mol mg}^{-1}\text{chlorophyll h}^{-1}$ in the WT and mutant, respectively. Chlorophyll contents were close to 400 mg m^{-2} in both plant types, so that carboxylation capacities would be approximately 34 (WT) and 45 (CMSII) $\mu\text{mol m}^{-2} \text{ s}^{-1}$. These rates are in reasonable agreement with light-dependent O_2 evolution measured under saturating conditions (Table I). Both types of measurement show that the maximum photosynthetic capacity of the mutant, on a leaf area basis, is at least as great as the WT.

There is no indication that the inhibition of photosynthesis is because of stomatal effects. During steady-state photosynthesis, the relationship between net CO_2 fixation and transpiration was identical in the two genotypes (Fig. 3; Table III) and in the early part of the induction period, net CO_2 fixation was markedly lower for a given rate of transpiration in the mutant (Fig. 2). The perturbation of photosynthesis, therefore, appears to be because of metabolic restrictions in the photosynthetic cell.

A possible metabolic explanation of the lower rates of photosynthesis in the mutant is a limitation on Suc synthesis by mitochondrial ATP production (Krömer et al., 1988). Although CMSII mitochondria are less efficient in ATP production (Sabar et al., 2000), sev-

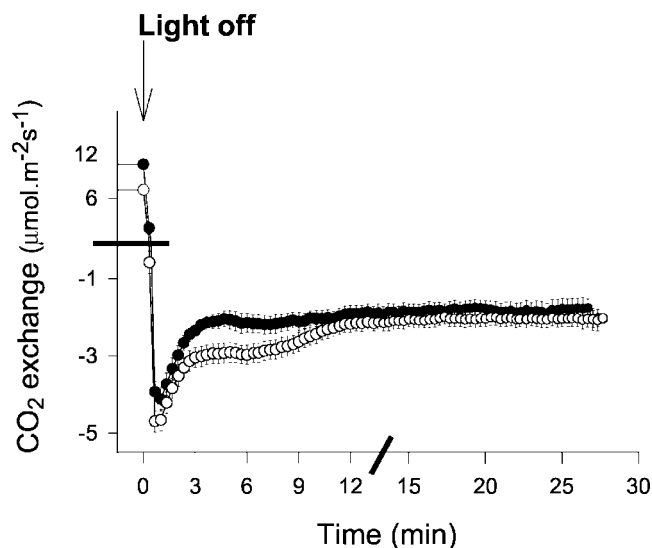


Figure 7. Analysis of postillumination CO_2 release in the WT tobacco and CMSII. Black circles, WT. White circles, CMSII. Gas exchange was analyzed in four different CMSII and WT plants. Attached leaves were illuminated at $1,000 \mu\text{mol m}^{-2} \text{ s}^{-1}$, $200 \mu\text{bar CO}_2$, and 210 mbar O_2 until the steady state was reached. Leaves were abruptly darkened and CO_2 evolution monitored. Data are means \pm SE of leaves from four different plants. Where not apparent, error bars are contained within the symbols. Note the discontinuous axis scaling, indicated by bars.

eral of our observations indicate that this is not the primary cause of the decreased photosynthetic activity. First, limitations of photosynthesis by triose phosphate utilization and associated phosphate recycling should be most evident when CO₂ and light are non-limiting, when there is a high demand on carbohydrate synthesis. This is consistent with effects of the mitochondrial ATPase inhibitor, oligomycin, on O₂ evolution by barley (*Hordeum vulgare*) protoplasts, where a more marked inhibition of photosynthesis was observed at high CO₂ (Krömer et al., 1993). In contrast, CMSII leaves evolved O₂ at least as fast as the WT when CO₂ was saturating (Table I) and the disruption of net CO₂ uptake was progressively mitigated by increasing ambient CO₂ (Figs. 3 and 4). Second, unlike the decreased photosynthesis in CMSII, which was independent of irradiance, the effect of oligomycin was observed preferentially at low and high light (Krömer et al., 1993). Third, O₂ sensitivity, which is decreased when carbohydrate synthesis limits CO₂ fixation (Leegood and Furbank, 1986; Sharkey et al., 1986), was even greater in CMSII than in the WT. Finally, the mutant does not have decreased leaf Suc contents (C. Dutilleul, R. De Paeppe, C.H. Foyer, and G. Noctor, unpublished data). Thus, the effect of complex I deficiency on leaf photosynthesis occurs via a different mechanism to that mediated by oligomycin treatment of protoplasts, and the observed effects cannot be explained purely in terms of a limitation by cytosolic ATP.

Complex I Plays an Important Role in Photorespiratory Metabolism in Vivo

It is still not clear to what extent the mitochondrial electron transport chain is involved in the oxidation of Gly in vivo. Redox shuttles operate between the mitochondria and cytosol (Ebbighausen et al., 1985) and during steady-state photorespiration, reduction of hydroxypyruvate in the peroxisomes requires NADH in amounts equal to that produced by the oxidation of Gly in the mitochondria (Leegood et al., 1995). However, isolated pea leaf mitochondria have been shown to preferentially oxidize Gly in the presence of other substrates (Dry et al., 1983; Douce and Neuburger, 1989), and glycerate synthesis can be supported by photosynthetic electron transport via export of reductant from the chloroplast (the so-called "malate valve," Backhausen et al., 1998; Backhausen and Scheibe, 1999). Adenylate measurements and inhibitor studies also suggest that Gly oxidation in illuminated leaves is at least partly coupled to the mitochondrial electron transport chain (Gärdeström and Wigge, 1988; Igamberdiev et al., 1997). From experiments with isolated pea and spinach (*Spinacia oleracea*) mitochondria, it was concluded that only 25% to 50% of the reducing equivalents from Gly oxidation is exported to the peroxisomes (Krömer and Heldt, 1991; Hanning and Heldt, 1993). Assum-

ing that leaf discs from the two genotypes do not differ significantly in their rate of uptake of Gly into photosynthetic cells, the data of Figure 6 show that complex I deficiency limits Gly metabolism in leaves in the dark, in agreement with the slower rates of Gly oxidation in isolated mitochondria from CMSII (Sabar et al., 2000). However, the present study found no evidence for direct perturbation of Gly to Ser conversion in the light. Relatively modest decreases in GDC capacity lead to increased Gly/Ser under conditions favoring photorespiration (Wingler et al., 1997; Heineke et al., 2001), but in our study Gly/Ser was very similar at a given rate of photosynthesis, whether the principal dehydrogenase of the mitochondrial electron transport chain was functional or not (Fig. 5). This compares with the massive disruption of Gly metabolism that we observed in the GDC-deficient barley mutant, LaPr87/30 (Blackwell et al., 1990), using a similar procedure and conditions (600 $\mu\text{mol m}^{-2} \text{s}^{-1}$ irradiance, 360 $\mu\text{bar CO}_2$, and 210 mbar O₂). In LaPr87/30, which has about 14% WT GDC activity, Gly/Ser increased to 66.4 ± 5.3 within 30 min illumination, whereas the ratio in WT barley at this point was 2.4 ± 0.1 (data not shown). The increased Gly/Ser in LaPr87/30 was not accompanied by a prolonged photosynthetic induction period, but rather by a progressive postinduction decline in net CO₂ uptake (data not shown). In stark contrast to these data, CMSII showed no increase in Gly/Ser over a wide range of photorespiratory flux. This observation, together with the substantial postillumination CO₂ burst in CMSII, shows that GDC is fully functional in this mutant and rules out the possibility that photosynthesis is inhibited because of inadequate capacity of this enzyme or to direct redox control over its activity. The similar relationship between Gly/Ser and the rate of photorespiration in the two genotypes suggests that sinks other than complex I are able to ensure adequate recycling of NADH produced by GDC in the light, and, thus, to mask the effect of complex I deficiency so that this effect is only apparent in the dark (Fig. 6). The slower oxidation of Gly in isolated mitochondria (Sabar et al., 2000) and in leaves in the dark suggests that these sinks are extra-mitochondrial, presumably hydroxypyruvate reduction with also, perhaps, a small contribution from nitrate reduction.

Even though the mutant showed no increase in Gly/Ser, complex I deficiency inhibited photosynthesis preferentially under photorespiratory conditions, when intercompartmental redox shuttles are very active. It is interesting to compare the relative rates of Gly metabolism in the two genotypes with their measured rates of leaf O₂ uptake in the dark. Rates of O₂ uptake of 1.3 (WT) and 2.1 (CMSII) $\mu\text{mol m}^{-2} \text{s}^{-1}$ (Table I) would be sufficient to support Gly metabolism at 5.2 and 8.4 $\mu\text{mol m}^{-2} \text{s}^{-1}$ in the WT and mutant, respectively. Using a simple model of C₃ photosynthesis (Novitskaya et al., 2002), it can be

calculated from typical photosynthetic rates observed in the two genotypes at atmospheric CO₂ and near-saturating light that rates of Gly formation would be 7.5 to 9 (WT) and 4.5 to 6 (CMSII) $\mu\text{mol m}^{-2} \text{s}^{-1}$. This comparison shows that photorespiration-dependent inhibition of photosynthesis in CMSII cannot be explained by decreased mitochondrial electron transport capacity. Rather, our data suggest that: (a) Gly oxidation in the WT in the light partly occurs through complex I; (b) in the absence of this enzyme Gly oxidation can be maintained by reductant export, i.e. the mitochondrial MDH and exchange transporters have sufficient capacity to avoid excessive increases in matrix NADH/NAD; but (c) the extra load on reductant sinks outside the mitochondria causes perturbation of redox distribution between subcellular compartments. Decreased photosynthesis in CMSII was most evident when net CO₂ fixation and photorespiration were both active, and was alleviated by suppressing photorespiration. Other studies have shown that decreased photorespiration is associated with a less reduced stroma (Backhausen and Scheibe, 1999), suggesting that extra-chloroplastic reductant sinks are particularly important under photorespiratory conditions. The observation that the decrease of steady-state photosynthesis is dependent on CO₂ and O₂, but independent of irradiance, shows that inhibition is not strictly dependent on absolute flux alone, but is also likely because of disruption of the stoichiometry of redox cycling. We will show elsewhere that leaf malate contents are increased in the mutant (C. Dutilleul, R. De Paepe, C.H. Foyer, and G. Noctor, unpublished data), possibly because of slower malate oxidation inside the mitochondria because of preferential use by GDC (Dry et al., 1983) of a more limited supply of NAD when complex I is not functional.

Redox Adjustment of Photosynthesis during Transients Requires Complex I Activity

Inhibitors of mitochondrial electron transport or oxidative phosphorylation have been shown to prolong the photosynthetic induction period in isolated protoplasts, both at suboptimal and saturating CO₂ (Igamberdiev et al., 1998; Padmasree and Raghavendra, 1999). Several explanations have been proposed to account for these observations, including limitations over ATP generation for Suc synthesis and perturbation of malate export from the chloroplast (Padmasree and Raghavendra, 1999; Gardeström et al., 2002). Our data show that complex I activity is required for rapid induction of photosynthesis specifically under photorespiratory conditions: Photosynthetic O₂ evolution was induced equally rapidly in the two genotypes at saturating CO₂ and slow induction of net CO₂ uptake was even more evident at low CO₂ than at atmospheric gas composition.

It can be inferred from the higher dark respiration rates in CMSII that complex I deficiency causes an

increased reduction state of NAD(P) in the cytosol and/or mitochondrion because substantial engagement of alternative dehydrogenases is likely to require increases in NADH or NADPH (Møller, 2001). Clear evidence that increased reduction of the stroma occurs in CMSII in the light comes from the observation that NADP-MDH activity remains high throughout the induction period of photosynthesis (Fig. 2). Redox poising is crucial during dark-light transitions (Foyer et al., 1992), and the malate valve may play a key role in this process, by linking chloroplast reductant supply to extra-chloroplastic sinks. In WT tobacco, the induction of NADP-MDH showed similar kinetics to those previously reported in pea leaves, where the initial rise and subsequent fall of activity during the induction period were shown to correlate tightly with leaf NADPH/NADP (Foyer et al., 1992). In CMSII, however, although rapidly induced, NADP-MDH remained high even when the rate of net CO₂ fixation approached that of the WT, suggesting an increased reduction state of the stroma because of insufficient electron sinks outside the chloroplast. Over-reduction of the photosynthetic system is also consistent with the pronounced second phase of postillumination CO₂ evolution in CMSII, which could reflect "light-enhanced dark respiration" (Reddy et al., 1991) possibly linked to a surplus of reducing equivalents in the light.

When supplied with malate and pyruvate, mitochondria from CMSII leaves showed similar O₂ consumption rates to WT mitochondria, though with a much lower sensitivity to rotenone (Sabar et al., 2000). Hence, increased reduction of the stroma does not result from a direct decrease in the mitochondrial capacity for malate oxidation in CMSII leaves because alternative dehydrogenases are able to compensate, at least in isolated mitochondria metabolizing malate in the presence of pyruvate. In illuminated leaves, however, where other substrates, notably Gly, are also generated, enhanced reduction of the stroma likely results from competition for a more limited number of regenerating sinks in CMSII and increased pressure on processes able to accept electrons from the malate valve (mitochondrial electron transport chain, peroxisomal glycerate synthesis, and cytosolic nitrate reduction). The corollary of this hypothesis is that glycerate synthesis is a significant sink for chloroplastic reductant, as suggested elsewhere (Hanning and Heldt, 1993; Hoefnagel et al., 1998).

Optimization of C₃ Photosynthesis in Physiological Conditions Requires Mitochondrial Complex I

The present data show that complex I is necessary to optimize photosynthesis when net CO₂ uptake and photorespiration are occurring simultaneously and during transients. Increased respiration through alternative dehydrogenases, the sustained activity of

NADP-MDH during the induction period, and the photorespiration-dependent inhibition of photosynthesis through a mechanism other than direct control over Gly oxidation, are all consistent with over-reduction of the photosynthetic system when complex I is deficient. The perturbation of photosynthesis in CMSII is not attributable to either insufficient photosynthetic or respiratory capacity, or to a direct block on Gly metabolism, but rather to disruption of redox distribution between the different subcellular compartments. Our data suggest that in the absence of complex I, the contribution of mitochondrial electron transport to Gly oxidation is decreased and the pressure on extra-mitochondrial sinks is increased, causing enhanced reduction of the chloroplast stroma and inhibition of photosynthesis. Thus, complex I is an indispensable component in WT plants when the photosynthetic cell has to simultaneously ensure reoxidation of malate and triose phosphate exported from the chloroplast and Gly produced in the mitochondria. During adjustment of the photosynthetic system to changes in irradiance, or to decreases in intercellular CO₂ that occur during the onset of drought (Cornic and Briantais, 1991), leaf complex I appears to be crucial in allowing an appropriate redox balance to be maintained, thereby avoiding the disruption of photosynthetic metabolism observed in CMSII.

MATERIALS AND METHODS

Plant Material and Growth Conditions

The experiments described were carried out at Rothamsted Research (Hertfordshire, UK). Tobacco (*Nicotiana sylvestris*) WT and the complex I-deficient mutant, CMSII (Gutierrez et al., 1997), were grown in 7-inch-diameter pots containing soil plus slow-release fertilizer in a controlled-environment greenhouse at 25°C (day) and 22°C (night). Illumination was provided by daylight supplemented by fluorescent lighting ensuring an irradiance of at least 200 to 300 $\mu\text{mol quanta m}^{-2} \text{s}^{-1}$ at the leaf surface (14-h day length). When the two lines had similar shoot and leaf size (7–10 weeks and 9–12 weeks after sowing for WT and CMSII, respectively), plants were transferred to the laboratory for measurements and sampling. All measurements were carried out on the youngest pair of fully expanded leaves.

O₂ Exchange Measurements

For each genotype, leaf discs (10 cm²) were excised and introduced into a leaf disc O₂ electrode chamber (Hansatech Instruments, Kings Lynn, Norfolk, UK). After calibration, the steady-state rate of O₂ consumption was monitored until a stable rate was reached. Discs were then illuminated at an irradiance of 1400 $\mu\text{mol m}^{-2} \text{s}^{-1}$ (22°C) until the steady-state rate of O₂ evolution was attained (within 10 min for both genotypes). The experiment was repeated with three different plants for each genotype.

Measurements of Steady-State CO₂ Exchange and Sampling for Metabolite Assays

Measurements of CO₂ and water exchange under steady-state conditions and sampling for metabolite analysis were performed as described by Novitskaya et al. (2002). All experiments were conducted at 22°C and 50% relative humidity. Irradiance was provided by overhead flood lamps and adjusted by neutral density sheeting. Gas composition was controlled by a gas mixer supplying CO₂ and O₂ to the stated partial pressures, with

balance N₂. Attached leaves from two mutant and two WT plants were analyzed simultaneously in multichamber systems linked to infrared gas analyzers. Respiratory CO₂ release was monitored for 20 min in the dark; then, plants were illuminated until a steady-state rate of CO₂ uptake was attained. To analyze the dependence of net CO₂ uptake on ambient CO₂ (Fig. 3), photosynthesis was induced at 360 $\mu\text{bar CO}_2$. CO₂ was then increased step wise from 70 to 1,000 μbar , and measurements were taken on attainment of the steady-state rate at each partial pressure. When gas exchange measurements were followed by sampling of the incubated portion of the leaf for determination of Gly/Ser (Fig. 4), each data point was necessarily obtained with a different leaf: Plants were pre-illuminated at 360 $\mu\text{bar CO}_2$ to induce photosynthesis; then, the CO₂ partial pressure was adjusted to the indicated value.

Amino Acid Measurements

To obtain the data for Ser and Gly shown in Figures 4 and 5 and Table III, sampling was performed in a four-chamber infrared gas analysis system in which two of the chambers measured WT leaves and two measured CMSII leaves. Experiments were performed twice at each condition to generate four replicates for each plant type. On attainment of the steady-state rate of photosynthesis, metabolism was stopped in the monitored part of the leaf by rapid-quench "freeze clamping" using precooled tongs mounted on rails attached to each chamber (Novitskaya et al., 2002). Samples were transferred into aluminum bags containing liquid N₂ and stored at -80°C until analysis. Leaf material was ground in N₂, then in absolute ethanol. An aliquot was set aside for chlorophyll determination at 654 nm, and the ethanol extract was diluted 1:1 (v/v) with water containing 120 μM α -aminobutyrate (internal standard). Extracts were incubated at 4°C for 30 min with regular mixing and clarified by centrifugation. Supernatant aliquots were dried under vacuum and amino acids determined by automated precolumn derivatization with *o*-phthalaldehyde, as in Novitskaya et al. (2002). Recovery quotients for amino acids added at the initial stage of the extraction were 99% \pm 2% (Gly) and 105% \pm 5% (Ser).

Gas Exchange and Sampling during Dark-Light and Light-Dark Transitions

For measurements of CO₂ exchange and transpiration during the induction period of photosynthesis, attached leaves were introduced into chambers as described above and darkened for 60 min. Leaves were then illuminated at 700 $\mu\text{mol m}^{-2} \text{s}^{-1}$, 210 mbar O₂, CO₂ partial pressure as indicated, and gas exchange was monitored until a steady-state rate of CO₂ uptake was reached. Samples for MDH assay were taken by freeze clamping at the times indicated.

For analysis of the postillumination burst of CO₂ release, attached leaves were illuminated at 1,000 $\mu\text{mol m}^{-2} \text{s}^{-1}$ at a gas composition of 210 mbar O₂ and 200 $\mu\text{bar CO}_2$. Once the steady-state rate of CO₂ uptake was attained, leaves were abruptly darkened and CO₂ exchange monitored using rapid-sampling software that allows acquisition of data every 2 s for a period of 25 min. The experiment was repeated with four WT plants and four CMSII plants.

Feeding Experiments

Leaf discs (5-mm diameter) were cut with cork borers from the lamina of six WT or CMSII leaves, each from a different plant. For each plant type, approximately 500 discs were placed directly on 5 mM HEPES (pH 7.0). Three replicate samples (one sample = eight discs sampled at random) were taken for amino acid analysis at time 0 and the remaining discs were divided between two large petri dishes, one containing 5 mM HEPES (pH 7.0) and the other 5 mM HEPES and 50 mM Gly (final pH adjusted to 7.0). Discs were incubated in the dark at 20°C. To ensure sufficient O₂ supply, air was gently bubbled through the solutions via syringe needles. Samples were taken at 3, 7, and 24 h after transfer of discs to the solutions. All sampling was carried out at very low light: Discs were transferred to a tea strainer, rinsed with deionized water, and blotted dry before freezing in liquid nitrogen. Samples were stored at -80°C until extraction of amino acids.

Enzyme Assays

For assay of Rubisco, attached leaves were introduced into the gas exchange chambers described above and either darkened for 5 h or illuminated at an irradiance of $700 \mu\text{mol m}^{-2} \text{s}^{-1}$ for 2 h. Samples were taken by freeze clamping, and stored at -196°C until extraction. Extraction and assays were performed using a method (P.J. Andralojc, personal communication) modified from Parry et al. (1997). This method measures three different Rubisco activities: initial activities, total activities (after preincubation to activate the enzyme), and maximal activities (after treatment to remove tight-binding inhibitors followed by preincubation to activate the enzyme). Leaf discs were ground in a precooled mortar into 0.575 mL of extraction buffer (50 mM Bicine-NaOH [pH 8.2], 20 mM MgCl_2 , 1 mM EDTA, 10 mM NaHCO_3 , 2 mM benzamidine, 5 mM ϵ -aminocaproic acid, 50 mM 2-mercaptoethanol, 10 mM dithiothreitol [DTT], and 2 mM phenylmethylsulfonyl fluoride) with 2% (w/v) insoluble polyvinylpyrrolidone. An aliquot was withdrawn for chlorophyll determination. The remainder was centrifuged for 3 min at 15,000g and 4°C . Aliquots of the supernatant were assayed for initial and total activities, and used for quantification of catalytic sites by binding of carboxyarabinitol bisphosphate as described below. To determine the maximal activity, 0.2 mL of supernatant was incubated for 30 min at 0°C in 0.2 M Na_2SO_4 and 10 mM NaHCO_3 . Rubisco was then precipitated by incubation for 30 min at 0°C with polyethylene glycol (PEG 4000) added to a final concentration of 25% (w/v), followed by centrifugation for 10 min at 12,000g and 4°C . The pellet was redissolved in 0.5 mL of 20% (w/v) PEG 4000 in 100 mM Bicine-NaOH (pH 8.2), 20 mM MgCl_2 , 10 mM NaHCO_3 , and 50 mM β -mercaptoethanol. After 10 min at 0°C , the precipitate was sedimented again and washed once more. The precipitate was then finally resuspended in 0.2 mL of extraction buffer and sonicated for 5 s. Aliquots of 25 μL and 0.2 mL were then taken for assay of maximal activity and quantification of catalytic sites, respectively. For all assays, 25 μL of sample was incubated at 25°C for 1 min in 0.475 mL of reaction buffer [100 mM Bicine-NaOH (pH 8.2), 20 mM MgCl_2 , and 10 mM $\text{NaH}^{14}\text{C}\text{CO}_3$ (0.5 $\mu\text{Ci} \cdot \mu\text{mol}^{-1}$)]. The reaction was started by addition of RuBP to a final concentration of 0.4 mM. To measure total and maximal activities, samples were preincubated for 3 min in the reaction buffer, before addition of RuBP, to fully carbamylate the enzyme. The assays were quenched by addition of 0.2 mL of 10 M formic acid, and then evaporated to dryness to remove all traces of acid-labile ^{14}C . After rehydration in 0.2 mL of water, the remaining ^{14}C was determined by liquid scintillation spectrometry. Total Rubisco catalytic sites were quantified by [^{14}C]carboxyarabinitol-1,5-bisphosphate (CABP) binding (Hall et al., 1981). Sample (0.15 mL) was added to 0.15 mL [^{14}C]CABP buffer [0.2 M Na_2SO_4 , 200 mM Bicine-NaOH (pH 8.2), 40 mM MgCl_2 , 20 mM NaHCO_3 , 100 mM β -mercaptoethanol, and 0.15 mM [^{14}C]CABP (1 $\mu\text{Ci} \cdot \mu\text{mol}^{-1}$)]. After 30 min at 0°C , Rubisco was precipitated by the addition of PEG 4000 to 25% (w/v). After further incubation for 30 min at 0°C , the precipitate was sedimented and washed as described above. The final pellet was resuspended in 0.5 mL of 1% (v/v) Triton X-100. [^{14}C]CABP was determined by liquid scintillation spectrometry. Rubisco activities were expressed relative to total Rubisco protein, and total catalytic sites were expressed relative to chlorophyll.

NADP-dependent MDH was extracted and assayed as in Trevanion et al. (1997). Frozen leaf tissue was ground in liquid N_2 and extracted into 25 mM HEPES-KOH (pH 7.5) buffer containing 10 mM MgSO_4 , 1 mM Na_2EDTA , 5 mM DTT, 1 mM phenylmethylsulfonyl fluoride, 5% (w/v) insoluble polyvinylpyrrolidone, and 0.05% (v/v) Triton X-100. After centrifugation for 5 min at 10,000g, the initial NADP-MDH activity was measured directly in the supernatant. To fully activate the enzyme, 0.2 mL of supernatant was preincubated for 30 min at 25°C in 40 mM Tricine-KOH (pH 9.0), 0.4 mM Na_2EDTA , 120 mM KCl, 100 mM DTT, and 0.0025% (v/v) Triton X-100. Assays were performed in 25 mM Tricine-KOH (pH 8.3), 150 mM KCl, 1 mM EDTA, 5 mM DTT, 0.2 mM NADPH, and 2 mM oxaloacetate, plus sample.

ACKNOWLEDGMENTS

We thank John Andralojc and Stephen Trevanion (Rothamsted Research, Hertfordshire, UK) for advice regarding the assays of Rubisco and MDH, respectively, Peter Lea (Lancaster University, UK) for the gift of barley LaPr87/30 seeds, and anonymous reviewers for constructive comments on the manuscript.

Received July 12, 2002; returned for revision August 18, 2002; accepted October 9, 2002.

LITERATURE CITED

- Backhausen JE, Emmerlich A, Holtgreffe S, Horton P, Nast G, Rogers JM, Müller-Röber B, Scheibe R (1998) Transgenic potato plants with altered expression levels of chloroplast NADP-malate dehydrogenase: interactions between photosynthetic electron transport and malate metabolism in leaves and in isolated intact chloroplasts. *Planta* **207**: 105–114
- Backhausen JE, Scheibe R (1999) Adaptation of tobacco plants to elevated CO_2 : influence of leaf age on changes in physiology, redox states and NADP-malate dehydrogenase activity. *J Exp Bot* **50**: 665–675
- Blackwell RD, Murray AJS, Lea PJ (1990) Photorespiratory mutants of the mitochondrial conversion of glycine to serine. *Plant Physiol* **94**: 1316–1322
- Cornic G, Briantais J-M (1991) Partitioning of photosynthetic electron flow between CO_2 and O_2 reduction in a C_3 leaf (*Phaseolus vulgaris* L.) at different CO_2 concentrations and during drought stress. *Planta* **183**: 178–184
- Douce R, Neuburger M (1989) The uniqueness of plant mitochondria. *Annu Rev Plant Physiol Plant Mol Biol* **40**: 371–414
- Dry IB, Day DA, Wiskich JT (1983) Preferential oxidation of glycine by the respiratory chain of pea leaf mitochondria. *FEBS Lett* **158**: 154–158
- Ebbighausen H, Chen J, Heldt HW (1985) Oxaloacetate translocator in plant mitochondria. *Biochim Biophys Acta* **810**: 184–199
- Foyer CH, Ferrario-Méry S, Noctor G (2001) Interactions between carbon and nitrogen assimilation. In PJ Lea, JF Morot-Gaudry, eds, *Plant Nitrogen*. Springer Verlag, Berlin, pp 237–254
- Foyer CH, Lelandais M, Harbinson J (1992) Control of the quantum efficiencies of photosystems I and II, electron flow, and enzyme activation following dark-to-light transitions in pea leaves. *Plant Physiol* **99**: 979–986
- Foyer CH, Noctor G (2000) Oxygen processing in photosynthesis: regulation and signalling. *New Phytol* **146**: 359–388
- Gardeström P, Igamberdiev AU, Raghavendra AS (2002) Mitochondrial functions in the light and significance to carbon-nitrogen interactions. In CH Foyer, G Noctor, eds, *Photosynthetic Nitrogen Assimilation and Associated Carbon and Respiratory Metabolism*, Advances in Photosynthesis, Vol 12. Kluwer Academic Press, Dordrecht, The Netherlands, pp 151–157
- Gardeström P, Wigge B (1988) Influence of photorespiration on ATP/ADP ratios in the chloroplast, mitochondria, and cytosol, studied by rapid fractionation of barley (*Hordeum vulgare*) protoplasts. *Plant Physiol* **88**: 69–76
- Gutiérrez S, Sabar M, Lelandais C, Chétrit P, Dioloz P, Degand H, Boutry M, Vedel F, De Kouchkovsky Y, De Paeppe R (1997) Lack of mitochondrial and nuclear-encoded subunits of complex I and alteration of the respiratory chain in *Nicotiana sylvestris* mitochondrial deletion mutants. *Proc Natl Acad Sci USA* **94**: 3436–3441
- Hall NP, Pierce J, Tolbert NE (1981) Formation of a carboxyarabinitol bisphosphate complex with ribulose bisphosphate carboxylase/oxygenase and theoretical specific activity of the enzyme. *Arch Biochem Biophys* **212**: 115–119
- Hanning I, Heldt HW (1993) On the function of mitochondrial metabolism during photosynthesis in spinach (*Spinacia oleracea* L.) leaves. *Plant Physiol* **103**: 1147–1154
- Heineke D, Bykova N, Gardeström P, Bauwe H (2001) Metabolic response of potato plants to an antisense reduction of the P-protein of glycine decarboxylase. *Planta* **212**: 880–887
- Hoefnagel MHN, Atkin OK, Wiskich JT (1998) Interdependence between chloroplasts and mitochondria in the light and the dark. *Biochim Biophys Acta* **1366**: 235–255
- Igamberdiev AU, Bykova NV, Gardeström P (1997) Involvement of cyanide-resistant and rotenone-insensitive pathways of mitochondrial electron transport during oxidation of glycine in higher plants. *FEBS Lett* **412**: 265–269
- Igamberdiev AU, Hurry V, Krömer S, Gardeström P (1998) The role of mitochondrial electron transport during photosynthetic induction. A study with barley (*Hordeum vulgare*) protoplasts incubated with rotenone and oligomycin. *Physiol Plant* **104**: 431–439
- Krömer S (1995) Respiration during photosynthesis. *Annu Rev Plant Physiol Plant Mol Biol* **46**: 45–70
- Krömer S, Heldt HW (1991) Respiration of pea leaf mitochondria and redox transfer between the mitochondrial and extramitochondrial compartment. *Biochim Biophys Acta* **1057**: 42–50

- Krömer S, Malmberg G, Gardeström P** (1993) Mitochondrial contribution to photosynthetic metabolism. A study with barley (*Hordeum vulgare* L.) leaf protoplasts at different light intensities and CO₂ concentrations. *Plant Physiol* **102**: 947–955
- Krömer S, Stitt M, Heldt HW** (1988) Mitochondrial oxidative phosphorylation participating in photosynthetic metabolism of a leaf cell. *FEBS Lett* **226**: 352–356
- Lambers H** (1997) Oxidation of mitochondrial NADH and the synthesis of ATP. In DT Dennis, DH Turpin, DD Lefebvre, DB Layzell, eds, *Plant Metabolism*. Addison Wesley Longman, Harlow, UK, pp 200–219
- Leegood RC, Furbank RT** (1986) Stimulation of photosynthesis by 2% oxygen at low temperatures is restored by phosphate. *Planta* **168**: 84–93
- Leegood RC, Lea PJ, Adcock MD, Häusler RE** (1995) The regulation and control of photorespiration. *J Exp Bot* **46**: 1397–1414
- Lewis CE, Noctor G, Causton D, Foyer CH** (2000) Regulation of assimilate partitioning in leaves. *Aust J Plant Physiol* **27**: 507–519
- Møller IM** (2001) Plant mitochondria and oxidative stress: electron transport, NADPH turnover, and metabolism of reactive oxygen species. *Annu Rev Plant Physiol Plant Mol Biol* **52**: 561–591
- Novitskaya L, Trevanion S, Driscoll S, Foyer CH, Noctor G** (2002) How does photorespiration modulate leaf amino acid contents? A dual approach through modelling and metabolite analysis. *Plant Cell Environ* **25**: 821–836
- Oliver DJ, Neuburger M, Bourguignon J, Douce R** (1990) Glycine metabolism by plant mitochondria. *Physiol Plant* **80**: 487–491
- Padmasree K, Raghavendra AS** (1999) Prolongation of photosynthetic induction as a consequence of interference with mitochondrial oxidative metabolism in mesophyll protoplasts of the pea (*Pisum sativum* L.). *Plant Sci* **142**: 29–36
- Pärnik T, Keerberg O** (1995) Decarboxylation of primary and end products of photosynthesis at different oxygen concentrations. *J Exp Bot* **46**: 1439–1447
- Parry MAJ, Andralojc PJ, Parmar S, Keys AJ, Habash D, Paul M, Alred R, Quick WP, Servaites JC** (1997) Regulation of Rubisco inhibitors in the light. *Plant Cell Environ* **20**: 528–534
- Reddy MM, Vani T, Raghavendra AS** (1991) Light-enhanced dark respiration in mesophyll protoplasts from leaves of pea. *Plant Physiol* **96**: 1368–1371
- Ruuska SA, Badger MR, Andrews JT, Von Caemmerer S** (2000) Photosynthetic electron sinks in transgenic tobacco with reduced amounts of Rubisco: little evidence for significant Mehler reaction. *J Exp Bot* **51**: 357–368
- Sabar M, De Paepe R, De Kouchkovsky Y** (2000) Complex I impairment, respiratory compensations, and photosynthetic decrease in nuclear and mitochondrial male sterile mutants of *Nicotiana sylvestris*. *Plant Physiol* **124**: 1239–1249
- Sharkey TD, Stitt M, Heineke D, Gerhard R, Raschke K, Heldt HW** (1986) Limitation of photosynthesis by carbon metabolism: II. O₂ insensitive CO₂ uptake results from limitation of triose phosphate utilization. *Plant Physiol* **81**: 1123–1129
- Somerville CR, Ogren WL** (1981) Photorespiration-deficient mutants of *Arabidopsis thaliana* lacking mitochondrial serine transhydroxymethylase activity. *Plant Physiol* **67**: 666–671
- Trevanion SJ, Furbank RT, Ashton AR** (1997) NADP-malate dehydrogenase in the C-4 plant *Flaveria bidentis*: cosense suppression of activity in mesophyll and bundle sheath cells and consequences for photosynthesis. *Plant Physiol* **113**: 1153–1165
- Vanlerberghe GC, Vanlerberghe AE, McIntosh L** (1994) Molecular genetic alteration of plant respiration: silencing and overexpression of alternative oxidase in transgenic tobacco. *Plant Physiol* **106**: 1503–1510
- Wingler A, Lea PJ, Leegood RC** (1997) Control of photosynthesis in barley plants with reduced activities of glycine decarboxylase. *Planta* **202**: 171–178